52nd IEEE Conference on Decision and Control
December 10-13, 2013. Florence, Italy

Cascade Sliding Mode-PID Controller for a Coupled-Inductor Boost Converter

Niliana Carrero, Carles Batlle and Enric Fossas, *Member, IEEE,*

***Abstract*—In this paper, a coupled-inductor Boost converter is modelled as a piece-wise complementarity system and controlled by means of two loops: a sliding mode control inner loop and an experimentally tuned PID outer loop control. The aim of the closed loop system is to regulate the output voltage of the coupled-inductor Boost converter. The control is carried out using the piece-wise complementarity model of the converter, which takes into account its hybrid dynamic. In addition, the performance and the effectiveness of the feedback control is validated through computer simulations using MATLAB and Psim.**

I. Introduction

In some emerging applications like fuel cells [1], wind power generation [2], photovoltaic systems [3], or lighting applications [4], the use of switching power converters allows to modify electrical power efficiently. However, power converter analysis and control design is not an easy task, because the key elements are active and passive switches (diodes), which possess piecewise-linear current/voltage characteristics [5] (voltages in diodes may be discontinuous).

Recently these switching networks have been modelled as linear complementarity systems [6]. Voltages at capacitors and currents through inductances are usually taken as state variables, while diode currents and voltages act as complementarity variables. The coupled-inductor boost converter considered in this paper can be described as a piece-wise linear complementarity system. It is locally modelled by two switching structures, which correspond to the converter models when the switch is in ON and OFF positions.

Several feedback techniques have been used to solve regulation or tracking problems in power converters. Linear control techniques are the most common, because its simplicity. Continuous controllers are synthesized for averaged models in a continuous-time framework and implemented through pulse width modulation (PWM). Since the averaged models result, in general, in non-linear dynamical systems, they are replaced by linearized systems at specific operating point regardless of any restrictions related to the control implementation. As a result, the controller design is valid in a neighbourhood of the operating point only, which leads to low performances during transients [7]. Moreover, performance and stability of such controllers are guaranteed only for one converter operation mode, even though the system may function in continuous (CCM) and discontinuous (DCM) conduction modes over the entire operating range.

Model predictive control (MPC) [8], passivity based control [9], [10], linear quadratic regulators (LQR) [11], sliding mode control (SMC) [12], [13] may be found among the non-linear control techniques applied to regulation or tracking problems in power converters. Sliding mode control (SMC) is particularly appropriate to control such converters since they intrinsically are discontinuous systems because of the switch [14]. V. Utkin [15] popularized SMC in Western countries in the late seventies. Since then, SMC has been applied to mechanical, electrical, chemical, ... plants. The success of this discontinuous feedback control technique is due to its robustness in presence of system parameters variations and model uncertainties, good performance, a reduced order dynamics designed by the engineer and because it is easy to implement. However, there are also some disadvantages such as chattering and the need for some sophisticated mathematical formulations. For details, the reader is referred to [16], [17]. Nevertheless, from the engineer's side, the choice of a suitable sliding surface is not an easy task.

In this paper, a sliding mode control for a coupled-inductor Boost converter is presented. To the authors' knowledge, it is the first reference in the literature of a piece-wise linear complementarity converter controlled by means of SMC. The switching action is governed through an hysteresis. This converter is especially interesting because it achieves high efficiency without requiring an extreme duty ratio [18]. An indirect feedback control with inner and outer loops is synthesized. The inner loop is a sliding mode current control loop, while the outer one is a PID controller that tunes the current reference to regulate the output voltage. This two-loop scheme is applied to the power converter, which is modelled as a piece-wise complementarity system [19].

Although Utkin's mathematical analysis for obtaining the ideal sliding dynamics cannot be strictly applied to the complementarity formulation of our system, the simulations in closed-loop demonstrate the effectiveness of the approach.

The paper is organized as follows. The dynamic model of the coupled-inductor Boost converter using the complementarity framework is described in Section II and the control law is

Work partially supported by Spanish CICYT projects DPI2010-15110 and DPI2011-25649

Niliana Carrero and Enric Fossas are with the Institute of Industrial and Control Engineering, Universitat Politècnica de Catalunya, ETSEIB, Av. Diagonal 647, 08028 Barcelona, Spain (niliana.andreina.carrero@upc.edu, enric.fossas@upc.edu)

Carles Batlle is with Department of Applied Mathematics 4 and Institute of Industrial and Control Engineering, Universitat Politècnica de Catalunya, EPSEVG, Av. V. Balaguer s/n 08800 Vilanova i la Geltrú, Spain (carles.batlle@upc.edu)

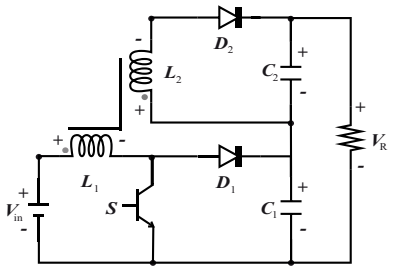

Fig. 1. Coupled-inductor Boost Converter

designed in Section III. The simulation results are in Section IV. Finally, some conclusions and considerations about further research are presented in Section V.

II. Coupled-Inductor Boost Converter

The circuit topology of the coupled-inductor Boost converter is shown in Fig 1. According to [6] the dynamics of the converter using linear complementarity systems (LCS) is given by

- S=On $(v_s = 0)$

$$\begin{aligned} \dot{x} &= A_1 x + B_1 \omega + E_1 V_{in} \\ z &= C_1 x + D_1 \omega + F_1 V_{in} \\ 0 &\leq z_1 \perp \omega_1 \geq 0 \\ 0 &\leq z_2 \perp \omega_2 \geq 0 \end{aligned} \tag{1}$$

and the pairs of complementary variables are given by

$$\begin{aligned} \omega_1 = i_{D1} \rightarrow z_1 = -v_{D1} = x_3 \\ \omega_2 = -v_{D2} \rightarrow z_2 = i_{D2} = x_2 \end{aligned} \tag{2}$$

with

$$\begin{aligned} A_1 &= \begin{pmatrix} 0 & 0 & 0 & M \\ 0 & 0 & 0 & -L_1 \\ 0 & 0 & -\Delta & -\Delta \\ 0 & 1 & -\Delta & -\Delta \end{pmatrix}, B_1 = \begin{pmatrix} 0 & M \\ 0 & -L_1 \\ -1 & 0 \\ 0 & 0 \end{pmatrix}, \\ E_1 &= \begin{pmatrix} L_2 \\ -M \\ 0 \\ 0 \end{pmatrix}, \quad C_1 = \begin{pmatrix} 0 & 0 & 1 & 0 \\ 0 & 0 & 0 & 1 \end{pmatrix}, \\ D_1 &= \begin{pmatrix} 0 & 0 \\ 0 & 0 \end{pmatrix}, \quad F_1 = \begin{pmatrix} 0 \\ 0 \end{pmatrix} \end{aligned} \tag{3}$$

- S=Off $(i_s = 0)$

$$\begin{aligned} \dot{x} &= A_2 x + B_2 \omega + E_2 V_{in} \\ z &= C_2 x + D_2 \omega + F_2 V_{in} \\ 0 &\leqslant z_1 \perp \omega_1 \geqslant 0 \\ 0 &\leqslant z_2 \perp \omega_2 \geqslant 0 \end{aligned} \tag{4}$$

and the complementary variables are given by the two pairs

$$\begin{aligned} \omega_1 = -v_{D1} \rightarrow z_1 = i_{D1} = x_1, \\ \omega_2 = -v_{D2} \rightarrow z_2 = i_{D2} = x_2, \end{aligned} \tag{5}$$

with

$$\begin{aligned} A_2 &= \begin{pmatrix} 0 & 0 & -L_2 & M \\ 0 & 0 & M & -L_1 \\ 1 & 0 & -\Delta & -\Delta \\ 0 & 1 & -\Delta & -\Delta \end{pmatrix}, B_2 = \begin{pmatrix} -L_2 & M \\ M & -L_1 \\ 0 & 0 \\ 0 & 0 \end{pmatrix}, \\ E_2 &= E_1, \quad C_2 = \begin{pmatrix} 1 & 0 & 0 & 0 \\ 0 & 1 & 0 & 0 \end{pmatrix}, \\ D_2 &= D_1, \quad F_2 = F_1 \end{aligned} \tag{6}$$

We use normalized continuous state variables $x_1 = \frac{\Gamma}{V_{in}} i_{L_1}$, $x_2 = \frac{\Gamma}{V_{in}} i_{L_2}$, $x_3 = \frac{1}{V_{in}} v_{C_1}$ and $x_4 = \frac{1}{V_{in}} v_{C_2}$. The variables i_{L_1} and i_{L_2} denote the inductors currents through L_1 and L_2 respectively, and the voltages across the capacitor C_1 and C_2 are represented by v_{C_1} and v_{C_2}. The diodes D_1 and D_2 are modelled as ideal diodes, and their current-voltage characteristics are expressed by the pair of complementary variables z and ω. This set of constraints is called "complementary conditions" (CC) [20]. These inequalities hold component-wise, and $\perp$ denotes the orthogonality between both vectors, so that z can be positive only if $\omega = 0$, and vice versa. The normalization of the state and time variables yields the following normalized parameters $k = L_1 L_2 - M^2$, $\tau = \frac{t}{\sqrt{kC_1}}$, $\Delta = \frac{\Gamma}{R}$, $\Gamma = \sqrt{\frac{k}{C_1}}$. Note that, with this normalization, the voltage of the input source V_{in} is equal to 1.

In compact form, the dynamics of the converter can then be rewritten as

$$\begin{aligned} \dot{x} &= A_2 x + B_2 \omega + E_2 V_{in} + (\mathrm{A}x + \mathrm{B}\omega + \mathrm{E}V_{in})\, u \\ z &= C_2 x + D_2 \omega + F_2 V_{in} + (\mathrm{C}x + \mathrm{D}\omega + \mathrm{F}V_{\mathrm{in}})\, u \\ 0 &\leqslant \omega \perp z \geqslant 0 \\ u &= \begin{cases} 1 & \rightarrow \quad \mathrm{S = On} \\ 0 & \rightarrow \quad \mathrm{S = Off} \end{cases} \end{aligned} \tag{7}$$

where $\mathrm{A} = A_1 - A_2$, $\mathrm{B} = B_1 - B_2$, $\mathrm{C} = C_1 - C_2$, $\mathrm{D} = D_1 - D_2$, $\mathrm{E} = E_1 - E_2$ and $\mathrm{F} = F_1 - F_2$.

III. Control desing

In general, the main objective of control in DC-DC converters is to regulate the output dc-voltage (V_R) to a given reference value (V_{ref}). This is to be achieved by the application of an appropriate feedback control law u, which will control the switched state. One major concern in the designing process is that regulation must be carried out in the presence of load disturbances and input voltage variations. In addition, it must take also into account the restrictions over the manipulated variable (duty cycle). In this context, the general control scheme for our coupled-inductor Boost converter is shown in Fig. 2. For the inner loop, a non-linear control strategy similar to sliding mode control is proposed, with the goal of controlling the fast dynamics of the converter (the inductors currents), and a PID controller is designed for the outer loop. This second loop will set the internal reference (I_{ref}) of the current loop and at the same time will regulate the output voltage V_R of the converter. In this control all state variables of the converter (inductor currents and capacitor voltages) are sensed.

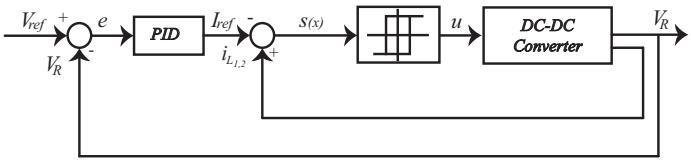

Fig. 2. Control scheme for the considered coupled-inductor Boost converter

A. Current control analysis

Assuming that the inductors currents in steady state have an average value, the purpose of the current control loop is to drive the average value of the inductors currents x_1 and x_2 to a reference value I_{ref}, and the sliding surface is defined as a linear combination of the state variables of the inductors currents given by

$$s(x) = L_1 x_1 + M x_2 - I_{ref}, \tag{8}$$

where I_{ref} is defined by the outer loop PID controller. The control action is designed as

$$u = \begin{cases} 0 & if \quad s(x) > 0, \\ 1 & if \quad s(x) < 0, \end{cases} \tag{9}$$

and, furthermore, a hysteretic function is added to the sliding function in order to maintain this near zero. Thus, using this control law, both existence and reaching conditions are being imposed to ensure the stability condition, at least in a neighborhood around the system equilibrium point. In the literature such condition is known as the reaching condition [15]. If the trajectories of the converter reach the vicinity of the sliding surface in which there is a sliding mode then they cannot leave that surface, except possibly at the boundaries of the sliding zone. This condition can be expressed mathematically as $\lim_{s\to 0^+} \dot{s} < 0$ and $\lim_{s\to 0^-} \dot{s} > 0$. These inequalities imply that in a neighborhood of $s(x)$, the function $s(x)$ evaluated on the trajectories of the system solution (7) is increasing for $s(x) < 0$ and decreasing for $s(x) > 0$. Thus, during the interval of time in which the switch is closed (On), one gets

$$\dot{s} = m_1 = L_1 L_2 - M^2. \tag{10}$$

Since in a coupled inductor the mutual inductance M has to be positive and lower than the geometric mean of the inductances of the coils, *i.e.* $0 \leqslant M \leqslant \sqrt{L_1 L_2}$, equation (10) implies that the derivative of $s(x)$ evaluated on the vector field (1) is positive. On the other hand, during the interval of time in which the switch is open (Off), one gets

$$\dot{s} = (L_1 L_2 - M^2)(1 + \omega_1 - x_3). \tag{11}$$

In this case the derivative of $s(x)$ depends on the complementarity variable ω_1, which is defined in (5). When $\omega_1 = 0$ one has

$$\dot{s} \equiv m_2 = (L_1 L_2 - M^2)(1 - x_3). \tag{12}$$

Since the output voltage x_3 must be greater than one, one has that, during the period of time in which $\omega_1 = 0$, the derivative of $s(x)$ is negative. In addition, it must also be negative when $\omega_1 \neq 0$ in order to guarantee sliding mode control. Indeed, in this case the inductor current is identically zero, $z_1 = i_{D_1} = x_1 = 0$, so its derivative is also zero during this period of time. Then, by replacing $\dot{x}_1 = 0$ in the expression $\dot{s} = L_1 \dot{x}_1 + M \dot{x}_2 = 0$ and using $\dot{x}_2$ from (4) one gets

$$\omega_1 = -\frac{L_2 + M x_4 - L_2 x_3}{L_2}. \tag{13}$$

Using this in (11) yields finally

$$\dot{s} \equiv m_3 = -\frac{M(L_1 L_2 - M^2) x_4}{L_2}. \tag{14}$$

Since the output voltage is $x_4 > 0$, the derivative during this period of time is also negative. Putting all the results together, one concludes that the reaching condition is satisfied.

Figure 3 provides the simulation results using the linear complementarity model (7) and under sliding mode control. As it can be observed from the surface trajectory s in Fig. 3(d), the existence and reaching conditions for having sliding modes on $s(x) = 0$ are satisfied. To the authors' knowledge, there is no definition of an equivalent control and its corresponding ideal sliding dynamics for general complementarity systems and, at present, we can only provide simulation results to validate the correctness of this modelling and control approach.

B. Voltage control analysis

The main goal of the voltage control loop is to regulate the output dc-voltage to a reference value. Thus, a discrete-time PID controller of the following form has been designed

$$C(z) = K_p + \frac{K_i T_s}{2} \frac{z+1}{z-1} + \frac{K_d}{T_s} \frac{z-1}{z}, \tag{15}$$

where K_p, K_i, K_d are the gain values of the controller and T_s is the sampling period. The parameters of this controller have been designed through experimental tuning according to different performance criteria such as minimal overshoot and shorter settling time. The values of the coefficients are $K_p = 1.4e-8$, $K_i = 1.1e-6$ and $K_d = 8e-12$ with $T_s = 50e-6$.

IV. Simulation results

The main purpose of this section is to show, through computer simulation, the effectiveness of the control law designed using the piece-wise complementarity model of the converter. In addition, simulations of the converter applying the control law designed using Psim where carried out. The simulations of the complementarity model given by equation (7) were performed using Matlab. The back-Euler method plus a specific solution of the linear complementarity problem (LCP) was used for the solution of the ordinary differential equations.

Two different scenarios of the closed loop system are presented. The first one takes into account a perturbation load and the second introduces step changes in the reference voltage.

- Scenario one: The nominal values of the converter parameters are $V_{in} = 12V$, $L_1 = 75\mu H$, $L_2 = 525\mu H$, $M = 196\mu H$, $C_1 = 22\mu F$, $C_2 = 22\mu F$, $R = 400\Omega$.

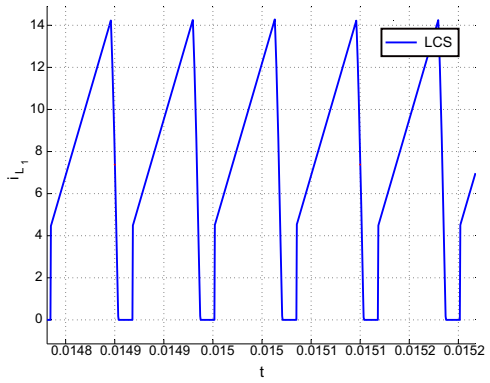

(a) Zoom of inductor current trajectory i_{L_1}

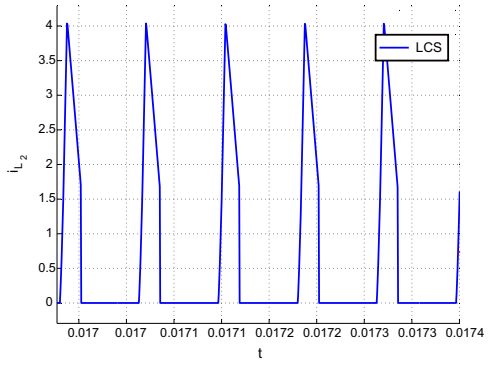

(b) Zoom of inductor current trajectory i_{L_2}

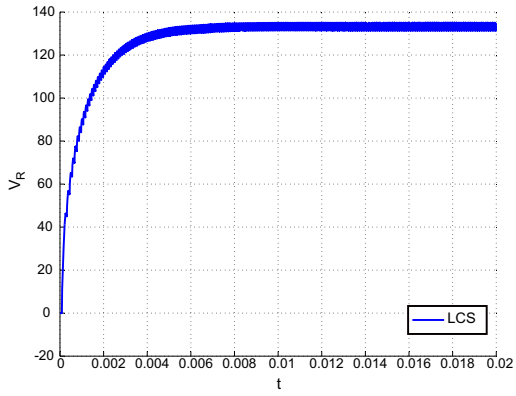

(c) Output voltage trajectory v_R

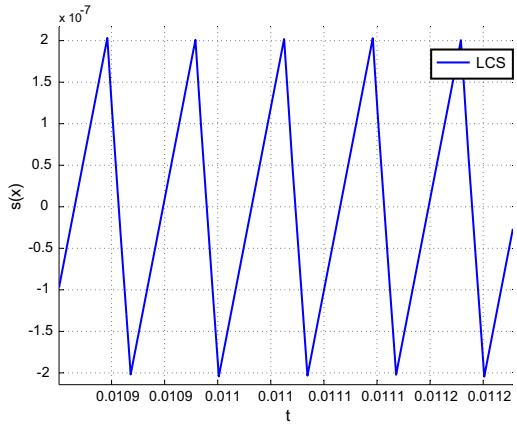

(d) Zoom of surface trajectory s

Fig. 3. Simulation result: current control

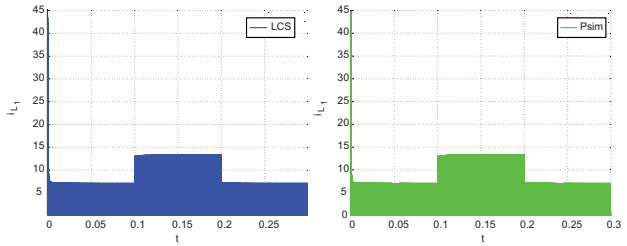

(a) Inductor current trajectory i_{L_1}

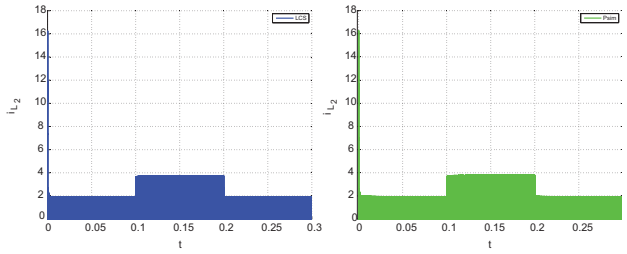

(b) Inductor current trajectory i_{L_2}

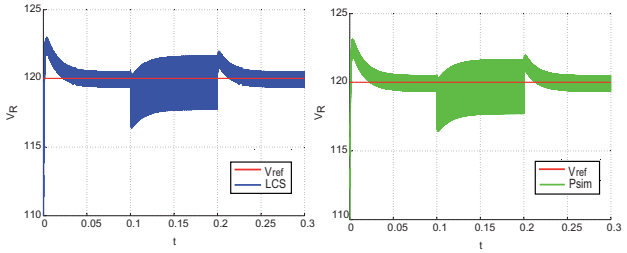

(c) Output voltage trajectory v_R

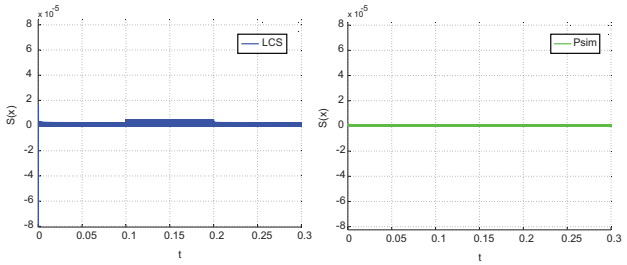

(d) Surface trajectory s

Fig. 4. Simulation results: load perturbation

The controller gains are $K_p = 1.4e-8$, $K_i = 1.1e-6$, $K_d = 8e-12$, and the hysteresis thresholds are $h_{max} = 6.20e-8$ and $h_{min} = -6.20e-8$. The controller goal is to regulate the output dc-voltage to a value $V_{ref} = 120V$. The initial conditions are $x(0) = [0,0,0,0]$. The waveforms of the inductors currents, output voltage and sliding surface trajectories are shown in Fig. 4. The left column corresponds to the complementarity model and the right one to the Psim model. As it can be observed from the simulation results, the output voltage V_R follows the reference. The robust tracking of the control law designed is made manifest when a change in the nominal value of the load from $R = 400\Omega$ to $R = 200\Omega$ is applied during the period of time

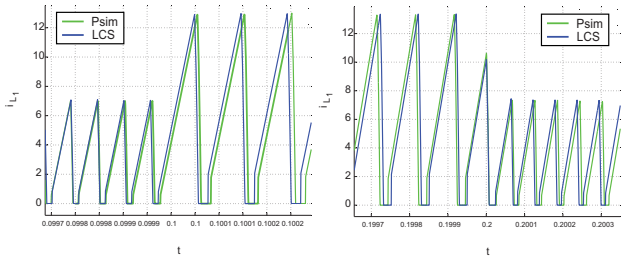

(a) Inductor current trajectory i_{L_1}

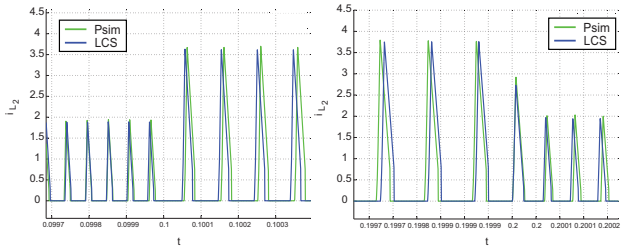

(b) Inductor current trajectory i_{L_2}

Fig. 5. Zoom of inductor currents trajectories

$0.1 < t < 0.2$. In Fig. 5(a) and Fig. 5(b) are shown a zoom of the inductors currents when a load perturbation has been applied. The left column corresponds to the time ($t = 0.1$) at which the load perturbation is applied, while the right column corresponds to the final time ($t = 0.2$).

- Scenario two: In this scenario, the nominal parameters are the same than in the load perturbation scenario, except for the load, which takes the value $R = 500\Omega$. The simulation results for the step reference changes are shown in Fig. 6. Just like before, the left column corresponds to the complementarity model and the right corresponds to the Psim model. The reference voltage is increased to $V_{ref} = 120V$ from its initial value $Vref = 80V$. This step reference is applied during the period of time $0.2 < t < 0.4$. Fig. 7(a) and Fig. 7(b) display a zoom of the inductor currents when the reference voltage is increased. The left column corresponds to the initial time ($t = 0.2$), while the right column corresponds to the final time ($t = 0.4$). It can be seen that there is a discrepancy between the Psim and complementarity models during the transient, although it disappears in the stationary regime. The results show that the controller is able to track this varying reference in an stable way.

V. Conclusions

A cascade control law has been applied to a coupled-inductor converter. It has been shown that excellent performance and stable tracking can be obtained with the proposed control law, which was tested using a piece-wise complementarity model of the converter, which takes into account its hybrid dynamics. The whole system was simulated in MATLAB. On the other hand, the same control law obtained

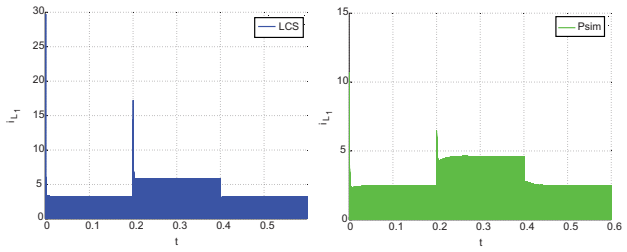

(a) Inductor current i_{L_1}

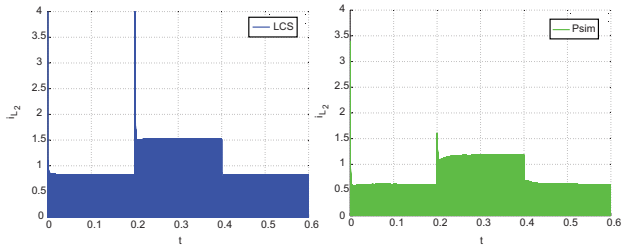

(b) Inductor current i_{L_2}

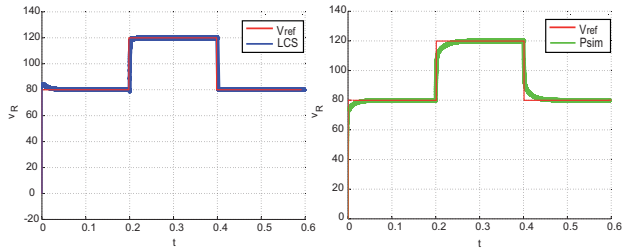

(c) Output voltage trajectory v_R

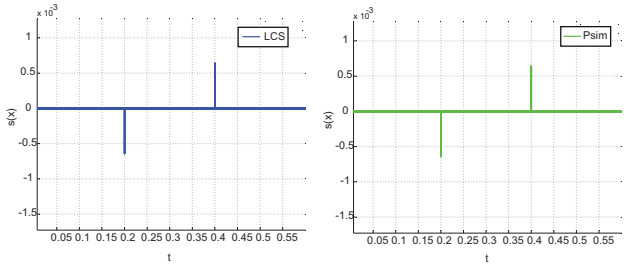

(d) Surface trajectory v_R

Fig. 6. Simulation result: step change in reference voltage

was applied to the model of the converter provided by Psim, showing negligible steady state discrepancies with the piece-wise complementarity model.

Besides being more faithful to the actual behaviour of the electronic components, the complementarity formulation allows for a systematic search of generalized discontinuous modes [20]. Furthermore, we have observed that, in specific simulations with the Psim model, increasing the switching frequency results in a loss of coupling inductances and, consequently, in a decrease of efficiency, while this does not happen with the complementarity-based Matlab model.

Future research will include experimental results for the specific converter discussed in this paper, and a general analysis of the ideal sliding dynamics for linear complementarity systems.

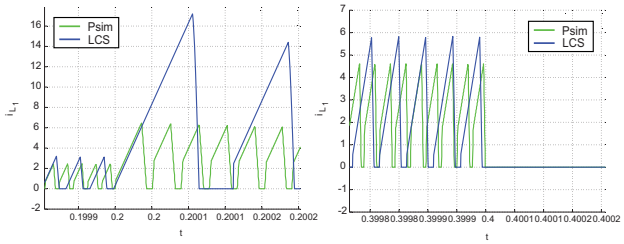

(a) Inductor current trajectory i_{L_1}

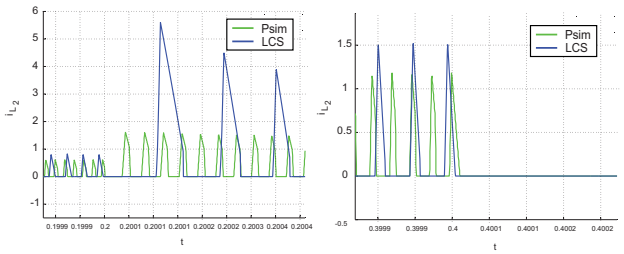

(b) Inductor current trajectory i_{L_2}

Fig. 7. Zoom of inductor currents trajectories

REFERENCES

[1] H.-H. Kim, H.-J. Lee, S.-C. Shin, Y.-S. Ko, M.-H. Shin, and C.-Y. Won, "Minimization of input current ripple in 2-level full-bridge converter for fuel cell power system," vol. 3, pp. 1910 –1914, june 2012.

[2] F. Blaabjerg, M. Liserre, and K. Ma, "Power electronics converters for wind turbine systems," in *Energy Conversion Congress and Exposition (ECCE), 2011 IEEE*, sept. 2011, pp. 281 –290.

[3] Y. Nishida, N. Aikawa, S. Sumiyoshi, H. Yamashita, and H. Omori, "A novel type of utility-interactive inverter for photovoltaic system," in *Power Electronics and Motion Control Conference, 2004. IPEMC 2004. The 4th International*, vol. 3, aug. 2004, pp. 1785 –1790 Vol.3.

[4] Y.-C. Chuang, Y.-L. Ke, H.-S. Chuang, and C.-C. Hu, "Single-stage power-factor-correction circuit with flyback converter to drive leds for lighting applications," in *Industry Applications Society Annual Meeting (IAS), 2010 IEEE*, oct. 2010, pp. 1 –9.

[5] R. W. Erickson and D. Maksimovic, *Fundamentals of power electronics*, 2nd ed., Springer, Ed. Kluwer academic publisehers, Marzo 2001.

[6] N. Carrero, C. Batlle, and E. Fossas, "Modeling a coupled-inductor boost converter in the complementarity framework," in *Computer Modeling and Simulation (EMS), 2012 Sixth UKSim/AMSS European Symposium on*, nov. 2012, pp. 471 –476.

[7] D. Patino and M. Baja, "Alternative control methods for dcdc converters: An application to a four-level three-cell dcdc converter," *International Journal of Robust and Nonlinear Control*, vol. 21, no. 10, pp. 1112–1133, July 2011.

[8] A. Wilson, P. Cortés, S. Kouro, J. Rodríguez, and H. Abu-Rub, "Model predictive control for cascaded h-bridge multilevel inverters with even power distribution," *Industrial Technology (ICIT), 2010 IEEE International Conference on*, pp. 1271–1276, 2010.

[9] B. Wang and Y. Ma, "Research on the passivity-based control strategy of buck-boost converters with a wide input power supply range," in *Power Electronics for Distributed Generation Systems (PEDG), 2010 2nd IEEE International Symposium on*, june 2010, pp. 304 –308.

[10] M. Perez, R. Ortega, and J. Espinoza, "Passivity-based pi control of switched power converters," *Control Systems Technology, IEEE Transactions on*, vol. 12, no. 6, pp. 881 – 890, nov. 2004.

[11] C. Olalla, R. Leyva, A. El Aroudi, and I. Queinnec, "Robust lqr control for pwm converters: An lmi approach," *Industrial Electronics, IEEE Transactions on*, vol. 56, no. 7, pp. 2548 –2558, july 2009.

[12] S.-C. Tan, Y. Lai, and C. Tse, "Indirect sliding mode control of power converters via double integral sliding surface," *Power Electronics, IEEE Transactions on*, vol. 23, no. 2, pp. 600 –611, march 2008.

[13] H. J. Sira-Ramirez and R. Silva-Ortigoza, *Control Design Techniques in Power Electronics Devices*, S. L. Ltd, Ed., 2006.

[14] D. Biel and E. Fossas, "Some experiments on chattering suppression in power converters," in *Control Applications, (CCA) Intelligent Control, (ISIC), 2009 IEEE*, july 2009, pp. 1523 –1528.

[15] V. Utkin, "Variable structure systems with sliding modes," *Automatic Control, IEEE Transactions on*, vol. 22, no. 2, pp. 212 – 222, apr 1977.

[16] L. Fridman, J. Moreno, and R. Iriarte, *Sliding Modes After the First Decade of the 21st Century: State of the Art Fridm*, ser. Lecture Notes in Control and Information Sciences. Springer Verlag, 2011, vol. 412.

[17] V. Utkin, J. Guldner, and J. Shi, *Sliding Mode Control in Electro-mechanical Systems (Automation and Control Engineering*, C. P. I. E. 2nd Revised edition, Ed., 2009.

[18] Q. Zhao and F. Lee, "High performance coupled-inductor dc-dc converters," in *Applied Power Electronics Conference and Exposition, 2003. APEC '03. Eighteenth Annual IEEE*, vol. 1, feb. 2003, pp. 109 – 113 vol.1.

[19] F. Vasca, G. Angelone, and L. Iannelli, "Linear complementarity models for steady-state analysis of pulse-width modulated switched electronic systems," in *Control Automation (MED), 2011 19th Mediterranean Conference on*, june 2011, pp. 400 –405.

[20] C. Batlle, E. Fossas, I. Merillas, and A. Miralles, "Generalized Discontinuous Conduction Modes in the Complementarity Formalism," *Circuits and Systems II: Express Briefs, IEEE Transactions on*, vol. 52, pp. 447–451, 2005.